Inorg. Chem. **2008**, *47*, 1224–1236

Direct Oxidation of L-Cysteine by $[Fe^{III}(bpy)_2(CN)_2]^+$ and $[Fe^{III}(bpy)(CN)_4]^-$

Xiaoguang Wang and David M. Stanbury*

Department of Chemistry and Biochemistry, Auburn University, Auburn, Alabama 36849

Received September 24, 2007

The oxidation of L-cysteine by the outer-sphere oxidants $[Fe(bpy)_2(CN)_2]^+$ and $[Fe(bpy)(CN)_4]^-$ in anaerobic aqueous solution is highly susceptible to catalysis by trace amounts of copper ions. This copper catalysis is effectively inhibited with the addition of 1.0 mM dipicolinic acid for the reduction of $[Fe(bpy)_2(CN)_2]^+$ and is completely suppressed with the addition of 5.0 mM EDTA (pH < 9.00), 10.0 mM EDTA (9.0 < pH ≤ 10.0), and 1.0 mM cyclam (pH > 10.0) for the reduction of $[Fe(bpy)(CN)_4]^-$. ^{1}H NMR and UV–vis spectra show that the products of the direct (uncatalyzed) reactions are the corresponding Fe(II) complexes and, when no radical scavengers are present, L-cystine, both being formed quantitatively. The two reactions display mild kinetic inhibition by Fe(II), and the inhibition can be suppressed by the free radical scavenger PBN (*N*-tert-butyl-α-phenylnitrone). At 25 °C and $\mu = 0.1$ M and under conditions where inhibition by Fe(II) is insignificant, the general rate law is $-d[Fe(III)]/dt = k[\text{cysteine}]_{tot}[Fe(III)]$, with $k = \{k_2K_{a1}[H^+]^2 + k_3K_{a1}K_{a2}[H^+] + k_4K_{a1}K_{a2}K_{a3}\{/\}[H^+]^3 + K_{a1}[H^+]^2 + K_{a1}K_{a2}[H^+] + K_{a1}K_{a2}K_{a3}\}$, where K_{a1}, K_{a2}, and K_{a3} are the successive acid dissociation constants of $HSCH_2CH(NH_3^+)CO_2H$. For $[Fe(bpy)_2(CN)_2]^+$, the kinetics over the pH range of 3–7.9 yields $k_2 = 3.4 \pm 0.6$ M^{-1} s^{-1} and $k_3 = (1.18 \pm 0.02) \times 10^6$ M^{-1} s^{-1} (k_4 is insignificant in the fitting). For $[Fe(bpy)(CN)_4]^-$ over the pH range of 6.1–11.9, the rate constants are $k_3 = (2.13 \pm 0.08) \times 10^3$ M^{-1} s^{-1} and $k_4 = (1.01 \pm 0.06) \times 10^4$ M^{-1} s^{-1} (k_2 is insignificant in the fitting). All three terms in the rate law are assigned to rate-limiting electron-transfer reactions in which various thiolate forms of cysteine are reactive. Applying Marcus theory, the self-exchange rate constant of the $^{\bullet}SCH_2CH(NH_2)CO_2^-/^-SCH_2CH(NH_2)CO_2^-$ redox couple was obtained from the oxidation of L-cysteine by $[Fe(bpy)(CN)_4]^-$, with $k_{11} = 4 \times 10^5$ M^{-1} s^{-1}. The self-exchange rate constant of the $^{\bullet}SCH_2CH(NH_3^+)CO_2^-/^-SCH_2CH(NH_3^+)CO_2^-$ redox couple was similarly obtained from the rates with both Fe(III) oxidants, a value of 6×10^6 M^{-1} s^{-1} for k_{11} being derived. Both self-exchange rate constants are quite large as is to be expected from the minimal rearrangement that follows conversion of a thiolate to a thiyl radical, and the somewhat lower self-exchange rate constant for the dianionic form of cysteine is ascribed to electrostatic repulsion.

Introduction

Thiol-containing compounds play important roles in biochemical processes, including maintaining cellular redox potentials, protecting cells against oxidative stress, and regulating metabolism and gene expression.[1−5] These processes can involve thiol/disulfide exchange, hydrogen atom transfer, or electron transfer.[3] The most important thiols in biological chemistry are cysteine, homocysteine, and glutathione. Cysteine, one of the essential α-amino acids and one of the simplest biological thiols, can undergo oxidation either by metal ions or by nonmetallic oxidants to form the corresponding sulfinic acid or disulfide, depending on the oxidative capability of the oxidant. One-electron oxidation of cysteine might provide one of the routes for it to function as an antioxidant preventing oxidative damage to DNA, lipids, and proteins.[2,6,7] Another reason for interest in understanding the mechanism of the oxidation of cysteine by metal complexes is that it may be beneficial in developing rapid and reliable sensing techniques for the detection of cysteine and other biological thiols.[8−10]

* Corresponding author. E-mail: stanbdm@auburn.edu.

(1) Arrigo, A.-P. *Free Radical Biol. Med.* **1999**, *27*, 936−944.
(2) Hand, C. E.; Honek, J. F. *J. Nat. Prod.* **2005**, *68*, 293−308.
(3) Jacob, C.; Giles, G. I.; Giles, N. M.; Sies, H. *Angew. Chem., Int. Ed.* **2003**, *42*, 4742−4758.
(4) Jones, D. P.; Go, Y.-M.; Anderson, C. L.; Ziegler, T. R.; Kinkade, J. M.; Kirlin, W. G. *FASEB J.* **2004**, *18*, 1246−1248.
(5) Moriarty-Craige, S. E.; Jones, D. P. *Ann. Rev. Nutr.* **2004**, *24*, 481−509.
(6) Darkwa, J.; Olojo, R.; Chikwana, E.; Simoyi, R. H. *J. Phys. Chem. A* **2004**, *108*, 5576−5587.
(7) Halliwell, B.; Gutteridge, J. M. C. *Lancet* **1984**, *323*, 1396−1397.

10.1021/ic701891m CCC: $40.75
Published on Web 01/05/2008

The oxidation of cysteine by metal cations or metal complexes has been widely investigated, and a variety of mechanisms has been proposed.[11−23] For metal-ion oxidants, such as V(V),[19] Cr(VI),[17] Fe(III),[21] a long-lived cysteine-metal ion (RS-M) complex was observed in the reactions. In principle, complications arising from complex formation can be avoided by use of substitution-inert (outer-sphere) metal oxidants, and there are a number of such reports, including oxidations by $[Ir^{IV}Cl_6]^{2-}$,[16] $[Co^{III}W_{12}O_{40}]^{5-}$,[11] $[Fe^{III}(CN)_6]^{3-}$,[12] $[Co_2(CN)_{10}(O)_2]^{5-}$,[14] $[Mo^{V}(CN)_8]^{3-}$,[15] and $[[(bpy)_2H_2ORu^{III}]_2O]^{4+}$.[23] Unfortunately, catalysis by trace levels of copper ions is ubiquitous in outer-sphere oxidations of thiols,[12,14,15,24−27] and the oxidations of cysteine by $[Fe^{III}(CN)_6]^{3-}$, $[Co_2(CN)_{10}(O)_2]^{5-}$, and $[Mo^{V}(CN)_8]^{3-}$ are known to be trace copper catalyzed; no catalysis has been reported for the reactions of $[Co^{III}W_{12}O_{40}]^{5-}$, $[Ir^{IV}Cl_6]^{2-}$, and $[[(bpy)_2H_2ORu^{III}]_2O]^{4+}$, but it is possible that the copper catalysis was overlooked by the investigators of these reactions. As a consequence, there is little reliable information on the uncatalyzed outer-sphere oxidation of cysteine.

We have recently shown that it is possible to obtain detailed data on direct (uncatalyzed) outer-sphere thiol oxidations by use of appropriate ligands to inhibit the copper-catalyzed pathways.[15,24,26,27] Our first reports described the oxidation of thioglycolate (TGA) by $[Ir^{IV}Cl_6]^{2-}$,[27] $[Mo^{V}(CN)_8]^{3-}$,[26] and $[Os^{III}(phen)_3]^{3+}$.[24] These reactions uniformly have rate-limiting steps where the thiolate form undergoes electron transfer to form the thiyl radical, but they differ in their ultimate sulfur-containing products, producing the disulfide and the sulfonic acid with Ir(IV), the disulfide alone with Mo(V), and the disulfide with $[Os(phen)_2(phen\text{-}TGA)]^{2+}$ with Os(III). A reasonably consistent treatment in terms of the cross-relationship of the Marcus theory was obtained for these three reactions. Our sole report on the oxidation of cysteine utilized $[Mo^{V}(CN)_8]^{3-}$ as the oxidant;[15] here, the rate-limiting steps likewise involve electron transfer from the thiolate forms, and the product is just the disulfide, cystine. Because of the −3 charge on the Mo(V) oxidant and the −2 charge on the fully deprotonated form of cysteine, this reaction is complicated by a significant dependence on the specific cation in the electrolyte used to maintain ionic strength. This specific salt effect introduces a degree of departure from the Marcus model of electron transfer.

In an effort to obtain further information about the diversity of products that can arise from outer-sphere oxidation of cysteine and to obtain kinetic data that are less affected by specific salt effects, two relatively weak oxidants bearing small charges, $[Fe^{III}(bpy)_2(CN)_2]^{+}$ and $[Fe^{III}(bpy)(CN)_4]^{-}$, were selected in the present study. These two oxidants are well-established as substitution-inert mild one-electron oxidants in aqueous soultion.[28−32] As is shown next, these two reactions met these objectives; moreover, they both showed kinetic inhibition by Fe(II), thus tightening the constraints on mechanistic proposals.

Experimental Procedures

Reagents and Solutions. Ferrous ammonium sulfate hexahydrate (Fisher), potassium cyanide (Fisher), 2,2′-bipyridyl (Aldrich), L-cysteine (Fluka), L-cystine (Aldrich), *N*-tert-butyl-α-phenylnitrone (PBN, Aldrich), cacodylic acid (Sigma), sodium phosphate monobasic monohydrate (J. T. Baker), sodium phosphate dibasic (MCB), sodium hydroxide (Fisher), D_2O (Aldrich), 3-(trimethylsilyl)-1-propanesulfonic acid, sodium salt (DSS, Aldrich), 5,5′-dithiobis-(2-nitrobenzoic acid) (DTNB, Aldrich), ammonium chloride (Fisher), sodium bicarbonate (J. T. Baker), sodium carbonate (Fisher), cupric sulfate pentahydrate (Fisher), nickel sulfate hexahydrate (Fisher), ferric nitrate nonahydrate (Fisher), ferrous sulfate heptahydrate (J. T. Baker), cobalt sulfate heptahydrate (Fisher), manganese sulfate monohydrate (Fisher), zinc sulfate heptahydrate (J. T. Baker), ammonium molybdate (Aldrich), ethylenediaminetetraacetic acid disodium salt dihydrate (abbreviated as EDTA hereafter, MCB), 2,6-pyridinedicarboxylic acid (abbreviated as dipic hereafter, Aldrich), 1,4,8,11-tetraazacyclotetradecane (cyclam, Aldrich), tetraphenylphosphonium chloride (Aldrich), chlorine gas (Matheson Gas Products, Inc.), acetic acid (Fisher), sulfuric acid (Fisher), nitric acid (Fisher), hydrochloric acid (Fisher), chloroform (Fisher), dimethyl sulfoxide (DMSO, Fisher), and Dowex 50W-X8 resin (J. T. Baker) were used without further purification.

Sodium perchlorate (Fisher), lithium perchlorate (GFS chemical Co.), and sodium triflate (Aldrich) were recrystallized from hot water; their stock solutions were standardized by running an aliquot through a cation-exchange column packed with Dowex 50W-X8 resin, then titrating by standardized NaOH aqueous solution. Sodium acetate trihydrate (Fisher) was recrystallized from hot water and dried in a vacuum desiccator. Chloroacetic acid (Fisher) was

(8) Munday, R.; Munday, C. M.; Winterbourn, C. C. *Free Radical Biol. Med.* **2004**, *36*, 757−764.
(9) Nekrassova, O.; Kershaw, J.; Wadhawan, J. D.; Lawrence, N. S.; Compton, R. G. *Phys. Chem. Chem. Phys.* **2004**, *6*, 1316−1320.
(10) White, P. C.; Lawrence, N. S.; Davis, J.; Compton, R. G. *Electroanalysis* **2002**, *14*, 89−98.
(11) Ayoko, G. A.; Olatunji, M. A. *Polyhedron* **1983**, *2*, 577−582.
(12) Bridgart, G. J.; Fuller, M. W.; Wilson, I. R. *J. Chem. Soc., Dalton Trans.* **1973**, 1274−1280.
(13) Bridgart, G. J.; Wilson, I. R. *J. Chem. Soc., Dalton Trans.* **1973**, 1281−1284.
(14) Ghosh, S. K.; Saha, S. K.; Ghosh, M. C.; Bose, R. N.; Reed, J. W.; Gould, E. S. *Inorg. Chem.* **1992**, *31*, 3358−3362.
(15) Hung, M.; Stanbury, D. M. *Inorg. Chem.* **2005**, *44*, 3541−3550.
(16) Kottapalli, K. K.; Adari, K. K.; Vani, P.; Govindan, S. K. *Trans. Met. Chem.* **2005**, *30*, 773−777.
(17) McCann, J. P.; McAuley, A. *J. Chem. Soc., Dalton Trans.* **1975**, 783−790.
(18) Olatunji, M. A.; Okechukwu, R. C. *Inorg. Chim. Acta* **1987**, *131*, 89−94.
(19) Payasi, A. P.; Sharma, K.; Sharma, V. K. *J. Indian Chem. Soc.* **1987**, *64*, 186−187.
(20) Shi, T.; Berglund, J.; Elding, L. I. *Inorg. Chem.* **1996**, *35*, 3498−3503.
(21) Sisley, M. J.; Jordan, R. B. *Inorg. Chem.* **1995**, *34*, 6015−6023.
(22) Stevens, G. D.; Holwerda, R. A. *Inorg. Chem.* **1984**, *23*, 2777−2780.
(23) Iyun, J. F.; Musa, K. Y.; Ayoko, G. A. *Indian J. Chem., Sect. A: Inorg., Bio-inorg., Phys., Theor. Anal. Chem.* **1996**, *35A*, 210−213.
(24) Hung, M.; Stanbury, D. M. *Inorg. Chem.* **2005**, *44*, 9952−9960.
(25) Mandal, S.; Bose, R. N.; Reed, J. W.; Gould, E. S. *Inorg. Chem.* **1996**, *35*, 3159−3162.
(26) Saha, B.; Hung, M.; Stanbury, D. M. *Inorg. Chem.* **2002**, *41*, 5538−5543.
(27) Sun, J.; Stanbury, D. M. *J. Chem. Soc., Dalton Trans.* **2002**, 785−791.
(28) Hubbard, C. D.; Bajaj, H. C.; van Eldik, R.; Burgess, J.; Blundell, N. J. *Inorg. Chim. Acta* **1991**, *183*, 1−7.
(29) Nichols, P. J.; Grant, M. W. *Aust. J. Chem.* **1989**, *42*, 1085−1101.
(30) Pelizzetti, E.; Mentasti, E.; Pramauro, E. *Inorg. Chem.* **1978**, *17*, 1181−1186.
(31) Stasiw, R.; Wilkins, R. G. *Inorg. Chem.* **1969**, *8*, 156−157.
(32) Wilkins, P. C.; Jacobs, H. K.; Johnson, M. D.; Gopalan, A. S. *Inorg. Chem.* **2004**, *43*, 7877−7881.

recrystallized from hot water and dried in a vacuum desiccator; stock solutions were titrated with a standardized NaOH aqueous solution.

Sodium dipicolinate dihydrate ($Na_2(C_7H_3NO_4)\cdot 2H_2O$) was synthesized by mixing an aqueous solution of dipic with 2 equiv of NaOH and then drying by rotary evaporation. The ^{1}H NMR spectrum of sodium dipicolinate in D_2O consists of an overlapping doublet and triplet at 7.99 ppm. The differential scanning calorimetry (DSC) plot of sodium dipicolinate has an endotherm just above 100 °C, the magnitude of which corresponds to a loss of two water molecules of hydration.

Distilled deionized water was obtained from a Barnstead NANO pure infinity ultrapure water system. All Fe(III) and L-cysteine solutions were prepared in deionized water just prior to use and purged with Ar or N_2 for at least 15 min prior to the reaction to prevent possible complications caused by O_2. Fe(III) solutions were kept in the dark to prevent any photochemical changes. The concentration of L-cysteine was determined spectrophotometrically with Ellman's reagent at pH 7.46.[33,34]

$[Fe^{II}(bpy)_2(CN)_2]\cdot 3H_2O$. This compound was prepared and characterized as described previously.[35] ^{1}H NMR (400 MHz/D_2O, δ/ppm vs DSS): 9.40 (d, $J = 6.5$, 2H), 8.36 (d, $J = 7.7$, 2H), 8.32 (d, $J = 8.0$, 2H), 8.09 (t, $J = 7.8$, 2H), 7.92 (t, $J = 7.8$, 2H), 7.60 (t, $J = 5.8$, 2H), 7.32 (d, $J = 6.0$, 2H), 7.21 (t, $J = 7.0$, 2H).

$[Fe^{III}(bpy)_2(CN)_2]NO_3\cdot 2H_2O$. This compound was prepared and characterized as described previously.[35]

Preparation of $K_2[Fe^{II}(bpy)(CN)_4]\cdot 3H_2O$. Schilt's method[36] was used to prepare $K_2[Fe^{II}(bpy)(CN)_4]\cdot 3H_2O$. ^{1}H NMR (400 MHz/$D_2O$, δ/ppm vs DSS): 9.32 (d, $J = 4.9$, 2H), 8.20 (d, $J = 7.6$, 2H), 7.94 (t, $J = 7.8$, 2H), 7.47 (t, $J = 6.7$, 2H).

Preparation of $Li[Fe^{III}(bpy)(CN)_4]\cdot 2.5H_2O$. $Li[Fe^{III}(bpy)(CN)_4]\cdot 2.5H_2O$ was prepared according to published procedures.[37] After addition of lithium perchlorate to the solution of $PPh_4[Fe^{III}(bpy)(CN)_4]\cdot H_2O$, an orange precipitate was collected by vacuum filtration and dried in a vacuum desiccator for 12 h. Yield of $Li[Fe^{III}(bpy)(CN)_4]\cdot 2.5H_2O$: 0.292 g (66%). Anal. calcd for $C_{14}FeH_{12.4}LiN_6O_{2.2}$: C, 46.32; H, 3.39; N, 23.17. Found: C, 46.37; H, 3.54; N, 22.90.

Methods. UV−vis and ^{1}H NMR spectra and stopped-flow kinetic data were obtained as described previously.[35] Cyclic voltammograms and Osteryoung square wave voltammograms (OSWV) were recorded at a scan rate of 100 mV/s as described previously;[35] data were obtained with a Ag/AgCl reference electrode and are reported relative to NHE by applying a correction of 0.205 V.[38] A 450 Corning pH/ion meter with a Mettler Toledo InLab 421 pH electrode was used for pH measurements. For all kinetics studies, the concentration of L-cysteine was at least 10 times greater than that of the Fe(III) complexes. Reactions were maintained at 25.0 °C under anaerobic conditions and monitored at 522 nm ($Fe^{II}(bpy)_2(CN)_2$, $\epsilon_{522} = 5.5 \times 10^3\ M^{-1}\ cm^{-1}$) and 482 nm ($[Fe^{II}(bpy)(CN)_4]^{2-}$, $\epsilon_{482} = 2.8 \times 10^3\ M^{-1}\ cm^{-1}$), and the rate constants were obtained by fitting the data with OLIS-supplied first-order functions. All apparent rate constants were the average of at least five runs with ±5% error or less. Nonlinear-least-squares computer programs (Datafit 8.1 and Prism 4.0c)[39,40] with relative weighting (weighting by $1/Y^2$) were used to fit the overall rate law to the values of k_{obs}. A Specfit/32 version 3.0.15 global analysis system was applied to simulate the reaction traces.[41]

Table 1. UV−vis Absorbance and Electrochemical Characteristics of the Iron Complexes in Aqueous Solution

			ϵ ($M^{-1}\ cm^{-1}$)		
compounds	band	λ_{max} (nm)	this work	lit. value[a]	$E_{1/2}$ (mV)[b]
$Fe^{II}(bpy)_2(CN)_2$	I	352	5.3×10^3		
	II	522	5.5×10^3	5800	
$[Fe^{III}(bpy)_2(CN)_2]NO_3$	I	394	1.2×10^3	1200	759 ± 2
	II	544	2.4×10^2	200	
$K_2[Fe^{II}(bpy)(CN)_4]$	I	346	3.4×10^3	3470	
	II	482	2.8×10^3	2880	
$Li[Fe^{III}(bpy)(CN)_4]$	I	375	1.5×10^3	1450	537 ± 2
	II	416	9.4×10^2	920	

[a] Refs 36 and 41. [b] $E_{1/2}$ vs NHE, at 22 °C and $\mu = 0.10$ M.

The concentration of copper impurities was determined by atomic absorption spectroscopy (AA 240 atomic absorption spectrometer). For the oxidation of 2.0×10^{-3} M L-cysteine by 5.0×10^{-5} M $[Fe^{III}(bpy)_2(CN)_2]^+$ at $\mu = 0.10$ M and pH 6.94, the concentration of copper cations in the product solution was 0.25 μM; for the oxidation of 2.0×10^{-3} M L-cysteine by 5.0×10^{-5} M $[Fe^{III}(bpy)(CN)_4]^-$ at $\mu = 0.10$ M and pH 9.94, the concentration of copper cation in the product solution was 0.22 μM, of which most of the copper was from the sodium perchlorate and sodium carbonate buffer.

Results

Characterization of the Iron Complexes. The UV−vis absorbance characteristics of the iron complexes are shown in Table 1 and, for $[Fe(bpy)_2(CN)_2]^{n+}$, in Figure S-1 (Supporting Information), in which the extinction coefficients are very close to previous reports.[36,42] The cyclic voltammograms of 0.1 mM $[Fe^{III}(bpy)_2(CN)_2]^+$ and $[Fe^{III}(bpy)(CN)_4]^-$ in 0.10 M $NaCF_3SO_3$ are nearly reversible, with $\Delta E_{p/p} = 67$ and 64 mV, respectively; the derived values of $E_{1/2}$ are in reasonable agreement with prior reports.[43−45] The OSWVs of 1.0 mM $[Fe^{III}(bpy)_2(CN)_2]^+$ and 0.70 mM $[Fe^{III}(bpy)(CN)_4]^-$ in 0.10 M $NaCF_3SO_3$ are consistent with their cyclic voltammetry (CV) results. The ^{1}H NMR spectra of $Fe^{II}(bpy)_2(CN)_2$ and $[Fe^{II}(bpy)(CN)_4]^{2-}$ are consistent with the structures of the compounds, and the spectrum of the former is in good agreement with the literature report.[46]

(33) Garman, A. J. *Non-radioactive Labeling*; Academic Press: San Diego, 1997; p 119.
(34) Riddles, P. W.; Blakeley, R. L.; Zerner, B. *Analyt. Biochem.* **1979**, *94*, 75−81.
(35) Wang, X.; Stanbury, D. M. *Inorg. Chem.* **2006**, *45*, 3415−3423.
(36) Schilt, A. A. *J. Am. Chem. Soc.* **1960**, *82*, 3000−3005.
(37) Lescouezec, R.; Lloret, F.; Julve, M.; Vaissermann, J.; Verdaguer, M. *Inorg. Chem.* **2002**, *41*, 818−826.
(38) Sawyer, D. T.; Sobkowiak, A.; Roberts, J. L. *Electrochemistry for Chemists*, 2nd ed.; John Wiley and Sons: New York, 1995; p 192.
(39) *Datafit 8.1*; Oakdale Engineering: Oakdale, PA, 2005.
(40) *Prism 4.0c*; GraphPad Software, Inc.: San Diego, 2005.
(41) Binstead, R. A.; Jung, B.; Zuberbuhler, A. D. *Specfit/32 Global Analysis System*, version 3.0; Marlborough, MA, 2000.
(42) Papula, L.; Horvath, O.; Papp, S. *J. Photochem. Photobiol., A* **1990**, *54*, 205−212.
(43) George, P.; Hanania, G. I. H.; Irvine, D. H. *J. Chem. Soc.* **1959**, 2548−2554.
(44) Schilt, A. A. *Anal. Chem.* **1963**, *35*, 1599−1602.
(45) Terretaz, S.; Becka, A. M.; Traub, M. J.; Fettinger, J. C.; Miller, C. J. *J. Phys. Chem.* **1995**, *99*, 11216−11224.
(46) Agarwala, B. V.; Ramanathan, K. V.; Khetrapal, C. L. *J. Coord. Chem.* **1985**, *14*, 133−137.

Table 2. Effect of Cu^{2+} and $dipic^{2-}$ on the Reaction of $[Fe^{III}(bpy)_2(CN)_2]^+$ with L-Cysteine[a]

$[Cu^{2+}]_{added}$ (μM)	[$dipic^{2-}$/dipic] (mM)	$t_{1/2}$ (s)
0.0	0.0	0.77
0.0	1.0	20
5.0	0.0	0.006
5.0	1.0	20
5.0	2.0	20

[a] [L-Cysteine]$_0 = 6.0 \times 10^{-4}$ M, [$Fe^{III}(bpy)_2(CN)_2^+$]$_0 = 5.0 \times 10^{-5}$ M, with 10.0 mM chloroacetate buffer (pH 3.60), at $\mu = 0.10$ M (0.092 M $NaCF_3SO_3$) and 25 °C.

Stability of the Oxidants in Aqueous Solution. Although cyanide ligands stabilize the +3 oxidation state of iron in $[Fe^{III}(bpy)_2(CN)_2]^+$ and $[Fe^{III}(bpy)(CN)_4]^-$, Papula et al. found that $[Fe^{III}(bpy)_2(CN)_2]^+$ is photoreduced to $Fe^{II}(bpy)_2(CN)_2$ with a slow rate under a mercury arc lamp at pH 7.0,[42] which is within the pH range of the present studies. Accordingly, we tested the stability of $[Fe^{III}(bpy)_2(CN)_2]^+$ by recording UV−vis spectra of 0.50 mM $[Fe^{III}(bpy)_2(CN)_2]^+$ in 10.0 mM chloroacetate buffer (pH 3.05) and 10.0 mM phosphate buffer (pH 7.98) and found that the absorbance in both buffers at 394 nm was constant over 3600 s. Moreover, no other indications of instability of the oxidants were obtained in the course of these studies.

Metal-Ion Catalysis. Tests for copper catalysis in the aqueous oxidation of L-cysteine by $[Fe^{III}(bpy)_2(CN)_2]^+$ and $[Fe^{III}(bpy)(CN)_4]^-$ were performed as follows. For the oxidation of 1.20×10^{-3} M L-cysteine by 5.0×10^{-5} M $[Fe^{III}(bpy)_2(CN)_2]^+$ at pH 4.76 (10.0 mM acetate buffer), in the presence of 0.092 M $NaCF_3SO_3$ ($\mu = 0.10$ M), the half-life is 0.36 s. With the addition of 5.0 μM $CuSO_4$, the rate of the reaction is so fast that it occurs within the deadtime of the instrument (~2 ms). In contrast, with the addition of 5.0 μM Zn^{2+}, Ni^{2+}, Fe^{2+}, Co^{2+}, Mn^{2+}, or Mo(VI), the half-life is hardly affected ($t_{1/2} =$ ~0.22 s for each reaction). For the oxidation of 2.60×10^{-3} M L-cysteine by 5.0×10^{-5} M $[Fe^{III}(bpy)(CN)_4]^-$ at pH 5.96 (10.0 mM cacodylate buffer), in the presence of 0.093 M $NaClO_4$, the half-life is 0.373 s; with the addition of 1.0 μM $CuSO_4$, the half-life of the reaction is only 0.025 s. These results clearly demonstrate that traces of copper ions are strongly catalytic in the oxidation of L-cysteine by $[Fe^{III}(bpy)_2(CN)_2]^+$ and $[Fe^{III}(bpy)(CN)_4]^-$.

As in our prior studies on thiol oxidation,[15,26] we found that copper catalysis in the oxidation of cysteine by $[Fe^{III}(bpy)_2(CN)_2]^+$ can be completely inhibited by the addition of 2,6-pyridinedicarboxylic acid (dipic). Specifically, for the oxidation of 6.0×10^{-4} M L-cysteine by 5.0×10^{-5} M $[Fe^{III}(bpy)_2(CN)_2]^+$ at pH 3.60 (10.0 mM chloroacetate buffer) and $\mu = 0.10$ M ($NaCF_3SO_3$), a 1:1 mixture of the disodium salt of dipic ($dipic^{2-}$) and dipic (1.0 mM) is sufficient to control the pH and inhibit copper catalysis, as shown in Table 2. For all subsequent kinetic studies, 1.0 mM $dipic^{2-}$/dipic (1:1, for pH < 4.0) and 1.0 mM $dipic^{2-}$ (for pH > 4.0) were added to inhibit the copper catalysis.

Unfortunately, for the oxidation of L-cysteine by the weaker oxidant $[Fe^{III}(bpy)(CN)_4]^-$, dipic is less effective as an inhibitor of copper catalysis as shown in Table S-1. Thus, at pH 6, copper catalysis is still significant with the addition of 1.0 mM $dipic^{2-}$, and while 2 mM dipic is sufficient to mask impurity copper catalysis, it is insufficient to mask catalysis by 1 μM Cu^{2+}. When the pH of the solution is 9.9, copper catalysis is not completely inhibited even with the addition of 5.0 mM $dipic^{2-}$, as shown in Table S-1 and by the abrupt termination in the kinetics traces shown in Figure S-2 (Supporting Information). Hence, alternative inhibitors were investigated.

Table 3. Effect of EDTA at pH 6 on the Reaction of $[Fe^{III}(bpy)(CN)_4]^-$ with L-Cysteine[a]

$[Cu^{2+}]_{added}$ (μM)	[EDTA] (mM)	$t_{1/2}$ (s)
0.0	0.0	0.37
1.0	0.0	0.025
0.0	2.0	20
0.0	5.0	20
1.0	2.0	20
1.0	5.0	19

[a] [L-Cysteine]$_0 = 2.60 \times 10^{-3}$ M, [$Fe^{III}(bpy)(CN)_4^-$]$_0 = 5.0 \times 10^{-5}$ M, with 0.093 M $NaClO_4$ and 10.0 mM cacodylate buffer (pH 5.96), at 25.0 °C.

Table 4. Effect of EDTA/Cyclam at High pH on the Reaction of $[Fe^{III}(bpy)(CN)_4]^-$ with L-Cysteine[a]

inhibitor	$[Cu^{2+}]_{added}$ (μM)	[$NaClO_4$] (M)	pH	$t_{1/2}$ (s)	k_{obs} (s^{-1})
EDTA	0.0	0.0	10.21	0.28	2.2
EDTA	0.25	0.0	10.22	0.25	*b*
cyclam[c]	0.0	0.099	10.98[d]	0.16	4.3
cyclam[c]	0.50	0.099	10.91[d]	0.15	4.3
cyclam[c]	0.0	0.090	11.90[e]	0.28	5.2
cyclam[c]	0.50	0.090	11.85[e]	0.24	5.2

[a] [L-Cysteine]$_0 = 5.0 \times 10^{-4}$ M, [$Fe^{III}(bpy)(CN)_4^-$]$_0 = 5.0 \times 10^{-5}$ M, with 10.0 mM EDTA or 1.0 mM cyclam, at 25.0 °C. [b] Nonpseudo-first order. [c] [Cyclam] = 1.0 mM. [d] [NaOH] = 1.0 mM. [e] [NaOH] = 10.0 mM.

In prior studies, we found that potential inhibitors such as EDTA were unsuitable because the amines are susceptible to direct oxidation. As is shown next, amine-based inhibitors can, however, be used with $[Fe^{III}(bpy)(CN)_4]^-$ because it is such a weak oxidant. The data in Table 3 show that EDTA is an excellent inhibitor at pH 6, with 2 mM EDTA being sufficient for complete inhibition of catalysis by 1 μM Cu^{2+}. Despite this improvement at pH 6, at pH 10.2, EDTA is not sufficiently effective, as shown by the data in Table 4. Cyclam, on the other hand (which binds Cu^{2+} more strongly),[47,48] is a highly effective inhibitor, even at pH 10 and 11. It is assumed that, at very high pH values, the fully deprotonated cyclam is coordinated to the copper(II) cation. The relatively high pK_a values of cyclam and its low solubility at low pH values limit its chelating efficiency at lower pH values.[49,50] In view of these factors, our subsequent kinetic studies with $[Fe^{III}(bpy)(CN)_4]^-$ were performed with 5.0 mM EDTA at pH ≤ 9.00, 10.0 mM EDTA at 9.00 < pH ≤ 10.0, and 1.0 mM cyclam at pH > 10.0 to inhibit trace copper catalysis.

(47) Kodama, M.; Kimura, E. *J. Chem. Soc., Dalton Trans.* **1977**, 1473−1478.
(48) Martell, A. E.; Smith, R. M.; Motekaitis, R. J. *NIST Critically Selected Stability Constants of Metal Complexes Database, 7.0*; U.S. Department of Commerce: Gaithersburg, MD, 2003.
(49) Josceanu, A. M.; Moore, P.; Rawle, S. C.; Sheldon, P.; Smith, S. M. *Inorg. Chim. Acta* **1995**, *240*, 159−168.
(50) Kodama, M.; Kimura, E. *J. Chem. Soc., Dalton Trans.* **1977**, 2269−2276.

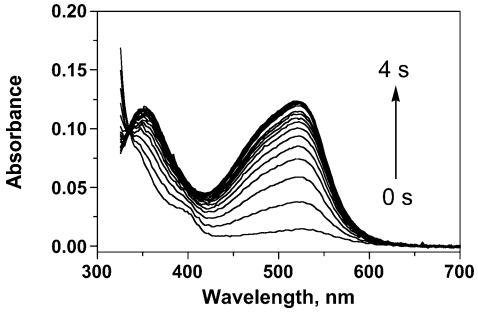

Figure 1. UV−vis spectra for the oxidation of 2.5×10^{-4} M L-cysteine by 2.5×10^{-5} M $[Fe^{III}(bpy)_2(CN)_2]^+$ at pH 6.02 (10.0 mM cacodylate buffer), with 1.0 mM dipic^{2-} at $\mu = 0.10$ M (0.093 M $NaCF_3SO_3$) and room temperature (time interval: 0.10 s). Data acquired with a rapid scanning Applied Photophysis SX-18MV stopped-flow instrument.

One concern raised by the use of amine-based inhibitors is that they could lead to catalysis by Fe^{2+} impurities (Fe-EDTA complexes) as has been shown in the oxidation of hydroxylamine by hexacyanoferrate(III).[51] Tests for this effect were performed under the following general conditions: 2.50×10^{-3} M L-cysteine, 5.0×10^{-5} M $[Fe^{III}(bpy)(CN)_4]^-$ at pH 5.90 (10.0 mM cacodylate buffer), with 0.093 M $NaCF_3SO_3$. The kinetics was monitored first with 1.0 mM EDTA, second with 1.0 mM EDTA and 1.0 μM $CuSO_4$, and third with 1.0 mM EDTA and 1.0 μM $Fe(NO_3)_3$. The rate constants for these three reactions were all within 10% of 0.030 s^{-1}, ruling out catalysis by Fe-EDTA.

As mentioned previously, another concern is that EDTA or cyclam might react directly with $[Fe^{III}(bpy)(CN)_4]^-$. To investigate this question, a solution of 1.0 mL of 5×10^{-5} M $[Fe^{III}(bpy)(CN)_4]^-$ and 1.0×10^{-3} M EDTA at pH 6.04 (10 mM cacodylate buffer) was monitored at 482 nm (455 nm optical cutoff filter), and no reaction was detected over 6000 s. The same experiment at pH 10.20 (10 mM carbonate buffer) yielded a slow reaction, with a rate constant of 3.0×10^{-3} s^{-1}. A very slow reaction was obtained with 1.0×10^{-3} M cyclam at pH 10.1, the half-life being longer than 2400 s. Since the cysteine reactions all occur on a much shorter time scale, EDTA and cyclam can be used safely as kinetic inhibitors in this reaction.

Stoichiometry: $[Fe^{III}(bpy)_2(CN)_2]^+$. Figure 1 shows repetitive scan UV−vis spectra for the direct oxidation of 2.5×10^{-4} M L-cysteine by 2.5×10^{-5} M $[Fe^{III}(bpy)_2(CN)_2]^+$ with 10.0 mM cacodylate buffer (pH 6.02), $\mu = 0.10$ M (0.093 M $NaCF_3SO_3$), and 1.0 mM dipic^{2-} at room temperature. With reference to the individual spectra of $[Fe^{III}(bpy)_2(CN)_2]^+$ and $[Fe^{II}(bpy)_2(CN)_2]$ (Figure S-1), Figure 1 shows the smooth conversion of $[Fe^{III}(bpy)_2(CN)_2]^+$ into $[Fe^{II}(bpy)_2(CN)_2]$, and the presence of a well-defined isosbestic point at 339 nm suggests that there is no accumulation of any long-lived iron-containing intermediate during the reaction.

The identity of the products was also determined by ^{1}H NMR spectroscopy. A sample was prepared as follows: equal volumes of 0.36 mM $[Fe^{III}(bpy)_2(CN)_2]^+$ and 2.0 mM L-cysteine in anaerobic D_2O were mixed in the presence of 1.0 mM dipic^{2-} and 1.0 mM DSS at pH 8.78 (adjusted by 1.0 M NaOD). Such low concentrations were dictated by the low solubility of the product cystine at this pH.[52,53] The ^{1}H NMR spectrum shown in Figure S-3 (Supporting Information) clearly reveals that L-cystine (3.91 (dd, $J = 7.9$, 4.1; 2H), 3.28 (dd, $J = 14.6$, 4.1; 2H), 3.07 (dd, $J = 14.5$, 8.0; 2H)) and $Fe^{II}(bpy)_2(CN)_2$ are the products of the reaction. The product stoichiometry of the reaction was determined by integration of the ^{1}H NMR spectrum, with Δ[Fe(II)]/Δ[L-cystine] being 1.5 ± 0.2. Unlike in the reaction of L-cysteine with octacyanomolybdate(V),[15] the ^{1}H NMR spectrum for the oxidation by $[Fe^{III}(bpy)_2(CN)_2]^+$ provides no evidence for the formation of L-cysteine-sulfinate.

Consumption ratios and product yields in the reaction between $[Fe^{III}(bpy)_2(CN)_2]^+$ and L-cysteine were also determined by spectrophotometric titration and analysis. Titration of 2.0 mL of 1.04×10^{-4} M L-cysteine by 5.09×10^{-3} M $[Fe^{III}(bpy)_2(CN)_2]^+$ at pH 7.61 was monitored at 522 nm, with 1.0 mM dipic^{2-} and 10 mM phosphate buffer. The consumption ratio of Δ[Fe(III)]/Δ[L-cysteine] was calculated from the titration curve that is shown in Figure S-4 (Supporting Information), with 1.12 ± 0.02 for Δ[Fe(III)]/Δ[L-cysteine]. Product yields were determined by mixing equal volumes of 0.40 mM deaerated L-cysteine and 0.20 mM $[Fe^{III}(bpy)_2(CN)_2]^+$ with 1.0 mM dipic^{2-} and 10.0 mM phosphate buffer (pH 6.94) in a bubbling flask for 10.0 min and then transferring the product solution to a stop-cocked cuvette. The concentration of $Fe^{II}(bpy)_2(CN)_2$ was determined from its characteristic absorbance at 522 nm, and the concentration of L-cysteine before and after the reaction was determined by the use of Ellman's reagent.[33,34] Given a reasonable estimate of $\pm$10% for the uncertainty in the molar absorptivity of Fe(II), the stoichiometric ratio, Δ[Fe(II)]/Δ[L-cysteine], was calculated as 1.0 ± 0.1, similar to the results obtained from spectrophotometric titrations.

The previous results imply that the overall reaction is

$$2[Fe^{III}(bpy)_2(CN)_2]^+ + 2\text{cysteine} \rightarrow 2Fe^{II}(bpy)_2(CN)_2 + \text{cystine} \quad (1)$$

The deviation from ideal stoichiometry obtained in the NMR product ratio is ascribed to the difficulties in obtaining accurate integrals with such dilute solutions.

Many of the kinetics experiments described next make use of the nitrone spin trap PBN to simplify the kinetic traces. A ^{1}H NMR spectrum of the product mixture at pH 3.10 in the presence of 0.10 mM PBN was recorded to determine the effect of PBN on the reaction stoichiometry. The spectrum (Figure S-5, Supporting Information) shows the products arising from a mixture of 0.20 mM $[Fe^{III}(bpy)_2(CN)_2]^+$ and 1.0 mM L-cysteine in D_2O, in the presence of 1.0 mM dipic. From 7.19 to 9.40 ppm, there are eight peaks with the same intensity, confirming the formation of $Fe^{II}(bpy)_2(CN)_2$. The chemical shifts at 4.00 and 3.09 ppm are due to excess L-cysteine, and the chemical shifts at 8.61 and 8.41 ppm are assigned as PBN (Figure S-6, Supporting

(51) Bridgart, G. J.; Waters, W. A.; Wilson, I. R. *J. Chem. Soc., Dalton Trans.* **1973**, 1582−1584.

(52) Apruzzese, F.; Bottari, E.; Festa, M. R. *Talanta* **2002**, *56*, 459−469.

(53) Sano, K. *Biochem. Z.* **1926**, *168*, 14−33.

Information) and the overlap of PBN with dipic^{2-}. The ratio of the integrated intensity of the chemical shift at 7.20 ppm (2H in $Fe^{II}(bpy)_2(CN)_2$) and 1.56 ppm (9H in tert-butyl in PBN) indicates that about 40% of the PBN was consumed in the reaction. The two singlets (at 1.33 and 2.05 ppm) are ascribed to products arising from the decomposition of the PBN-cysteinyl radical adduct.[54] Notably, no L-cystine is evident in the ^{1}H NMR spectrum, as is to be expected if the oxidation products are derived from the PBN-cysteinyl radical adduct. The consumption ratio for the reaction was obtained from the integrated intensities of the ^{1}H NMR spectrum, from which Δ[L-cysteine]/Δ[Fe(III)] = 1.0 ± 0.2. The reaction implied by these data at pH 3.1 is

$$[Fe^{III}(bpy)_2(CN)_2]^+ + \text{cysteine} + \text{PBN} \rightarrow Fe^{II}(bpy)_2(CN)_2 + \text{products} \quad (2)$$

The effect of PBN at higher pH values is rather different. At pH 8.7, the ^{1}H NMR spectrum for the oxidation of 1.0 mM L-cysteine by 0.20 mM $[Fe^{III}(bpy)_2(CN)_2]^+$ in D_2O, in the presence of 1.0 mM dipic^{2-}, 0.50 mM PBN, and 1.0 mM DSS, is shown in Figure S-7 (Supporting Information) and indicates that the products of the reaction are $Fe^{II}(bpy)_2(CN)_2$ and L-cystine. The concentration of PBN decreases by about 16% during the reaction, much less than in acidic solution. The stoichiometric ratio was obtained from the integrated intensities of the ^{1}H NMR spectrum, from which Δ[Fe(II)]/Δ[L-cystine] = 1.82 ± 0.07. Thus, at pH 8.7, PBN does not participate in the reaction, and eq 1 describes the stoichiometry. Likewise, spectrophotometric titration at pH 7.6 (shown in Figure S-8, Supporting Information) yields Δ[Fe(II)]/Δ[L-cysteine] = 1.13 ± 0.09, consistent with the NMR results at pH 8.7.

Stoichiometry: $[Fe^{III}(bpy)(CN)_4]^-$. The products of the reaction were investigated by ^{1}H NMR spectroscopy. Equal volumes of 0.80 mM $[Fe^{III}(bpy)(CN)_4]^-$ and 4.0 mM L-cysteine were mixed in anaerobic D_2O, in the presence of 1.0 mM cyclam and 2.0 mM DSS at pH 11.1 (adjusted by 0.10 M NaOD). The ^{1}H NMR spectrum of the product solution (Figure S-9, Supporting Information) clearly shows that L-cystine and $[Fe^{II}(bpy)(CN)_4]^-$ are the products of the reaction and that there is no evidence for the formation of L-cysteine-sulfinate. The stoichiometry of the reaction was determined by the quantitative analysis of the ^{1}H NMR spectra of the products, with Δ[Fe(II)]/Δ[L-cystine] = 1.97 ± 0.03.

The stoichiometry of the reaction between $[Fe^{III}(bpy)(CN)_4]^-$ and L-cysteine in the presence of EDTA was determined by spectrophotometric analysis as well. Two experiments were performed. Equal volumes of either 0.50 or 1.0 mM deaerated L-cysteine and 0.30 mM $[Fe^{III}(bpy)(CN)_4]^-$, with 5.0 mM EDTA and 10.0 mM ammonia buffer (pH 8.78), were mixed together in a bubbling flask for 10.0 min, and then the product solution was transferred to a stop-cocked cuvette. The concentration of $[Fe^{II}(bpy)(CN)_4]^{2-}$ was determined from its characteristic absorbance at 482 nm, and the concentration of L-cysteine before and after reaction was determined by Ellman's reagent.[33,34] The stoichiometric ratio, Δ[Fe(II)]/Δ[L-cysteine], was 1.28 ± 0.04 with 0.50 mM cysteine and 1.05 ± 0.04 with 1.0 mM cysteine. These results imply that some overoxidation might occur when the concentration of L-cysteine is slightly higher than that of $[Fe^{III}(bpy)(CN)_4]^-$, but the overoxidation becomes negligible at higher cysteine concentrations.

On the basis of these results, the overall reaction with a substantial excess of cysteine is

$$2[Fe^{III}(bpy)(CN)_4]^- + 2\text{cysteine} \rightarrow 2[Fe^{II}(bpy)(CN)_4]^{2-} + \text{cystine} \quad (3)$$

Kinetics: $[Fe^{III}(bpy)_2(CN)_2]^+$. Figure 2 shows a typical kinetic trace for the direct oxidation of 1.25 × 10^{-3} M L-cysteine by 2.5 × 10^{-5} M $[Fe^{III}(bpy)_2(CN)_2]^+$, with 10.0 mM chloroacetate buffer (pH 3.20), μ = 0.10 M (0.093 M $NaCF_3SO_3$), and 1.0 mM dipic^{2-}/dipic (1:1). Figure 2 shows the production of Fe(II) with $t_{1/2}$ = 37 s but with significant deviations from pseudo-first-order kinetics, and the character of the deviations is typical of product inhibition. Precipitation of cystine is not the cause of these deviations because the solubility of cystine greatly exceeds the oxidant concentration.[52,53] Tests for inhibition by Fe(II) were performed by adding 2.5 × 10^{-5} and 1.0 × 10^{-4} M $Fe^{II}(bpy)_2(CN)_2$ with the conditions being otherwise as stated previously: these additions significantly slowed the reactions, the half-lives being 52 and 90 s, respectively, as shown in Table 5. These results confirm that the deviations from pseudo-first-order kinetics are a consequence of inhibition by Fe(II).

The radical scavenger PBN proved to be effective in preventing inhibition by Fe(II). For example, essentially perfect pseudo-first-order kinetics was obtained with 0.1 mM PBN in the reaction of 1.25 × 10^{-3} M L-cysteine with 2.5 × 10^{-5} M $[Fe^{III}(bpy)_2(CN)_2]^+$ at pH 3.20 (10.0 mM chloroacetate buffer), with 1.0 mM dipic^{2-}/dipic (1:1) at μ = 0.10 M (0.093 M $NaCF_3SO_3$). As summarized by the data in Table 5, 0.1 mM PBN was also sufficient to prevent inhibition by 25 μM added Fe(II). A small degree of inhibition occurred with the addition of 100 μM Fe(II), but this effect was minimized by increasing the PBN concentration to 0.2 mM. Increasing the PBN concentration to 0.5 or 1.0 mM with no added Fe(II) led to no further changes in the kinetics. The effects of Fe(II) inhibition are less significant at higher pH values. Thus, at pH 4.6, only minor deviations from exponential kinetics are observed when PBN is omitted, and in its presence, the half-lives are only marginally decreased (Table S-2, Supporting Information). At pH 7.6, the kinetic traces give excellent exponential fits even without the addition of PBN, and the addition of as much as 0.5 mM PBN had no significant effect on the kinetics.

Unexpectedly, at pH 7.6, the rate constant decreased by 25% as the concentration of PBN increased from 0.5 to 7.5 mM (Table S-2). Recently, Potapenko et al. reported that the nitrone spin trap 5-diethoxyphosphoryl-5-methyl-1-pyrroline *N*-oxide (DEPMPO) is nucleophilically attacked

(54) Graceffa, P. *Biochim. Biophys. Acta* **1988**, *954*, 227−230.

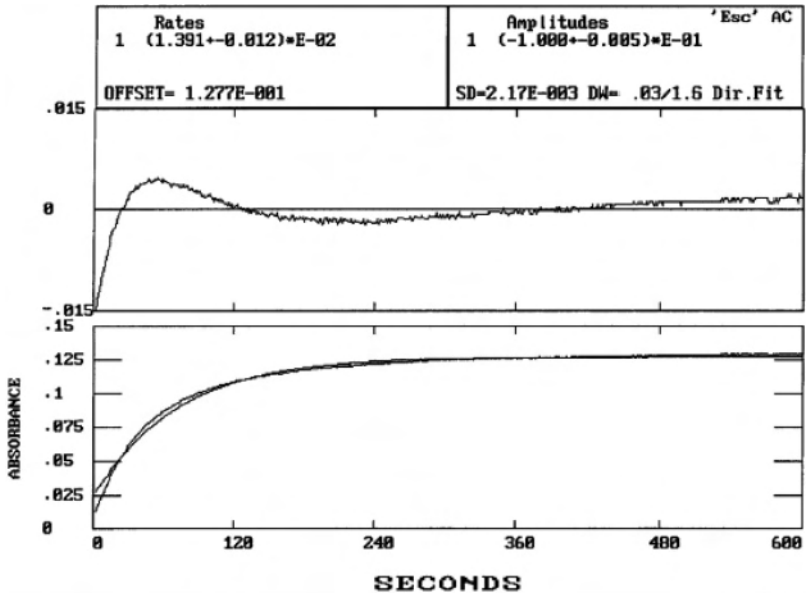

Figure 2. Reaction trace showing deviations from pseudo-first-order kinetics in the oxidation of 1.25×10^{-3} M L-cysteine by 2.5×10^{-5} M $[Fe^{III}(bpy)_2(CN)_2]^+$ at pH 3.20 (10.0 mM chloroacetate buffer), with the addition of 1.0 mM $dipic^{2-}$/dipic (1:1) at $\mu = 0.10$ M (0.093 M $NaCF_3SO_3$) and 25.0 °C.

Table 5. Effect of $Fe^{II}(bpy)_2(CN)_2$ and PBN on the Oxidation of L-Cysteine by $[Fe^{III}(bpy)_2(CN)_2]^+$ at pH 3.2[a]

$[Fe^{II}(bpy)_2(CN)_2]_0$ (mM)	[PBN] (mM)	$t_{1/2}$ (s)	k_{obs} (s^{-1})
0.00	0.00	37	*b*
0.025	0.00	52	*b*
0.10	0.00	90	*b*
0.00	0.10	36	1.9×10^{-2}
0.025	0.10	40	1.7×10^{-2}
0.10	0.10	53	1.3×10^{-2}
0.00	0.20	35	2.0×10^{-2}
0.025	0.20	38	1.8×10^{-2}
0.10	0.20	47	1.5×10^{-2}
0.00	0.50	35	0.020
0.00	1.0	34	0.021

[a] $[\text{L-Cysteine}]_0 = 1.25 \times 10^{-3}$ M, $[Fe^{III}(bpy)_2(CN)_2^+]_0 = 2.5 \times 10^{-5}$ M, pH 3.20 (10 mM chloroacetate buffer), $\mu = 0.10$ M ($NaCF_3SO_3$), $[dipic^{2-}/dipic] = 1.0$ mM, $\mu = 0.10$ M ($NaCF_3SO_3$). [b] Non-first-order.

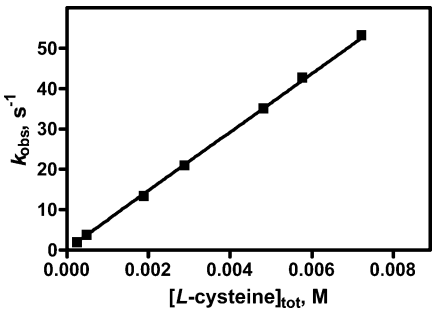

Figure 3. k_{obs} vs $[\text{L-cysteine}]_{tot}$ for the oxidation of L-cysteine by $[Fe^{III}(bpy)_2(CN)_2]^+$ at pH 6.0 (10.0 mM cacodylate buffer), with 1.0 mM $dipic^{2-}$ and 0.20 mM PBN at $\mu = 0.10$ M (0.093 M $NaCF_3SO_3$) and 25.0 °C, $[Fe^{III}(bpy)_2(CN)_2^+]_0 = 2.5 \times 10^{-5}$ M. Solid line is a linear fit, weighted by $1/Y^2$.

by L-cysteine to form DEPMPO hydroxylamine derivatives with an equilibrium constant of 0.03 M^{-1}.[55] To test as to whether a similar reaction occurs between cysteine and PBN (also a nitrone), we recorded the absorbance of 7.5 mM PBN at 326 nm after adding 5 mM cysteine at pH 7.6 (phosphate buffer). The absorbance decreased by 3% with a half-life of about 100 s, consistent with the approach to a small equilibrium conversion to a PBN/cysteine adduct. At lower cysteine concentrations, the absorbance change was too small to make accurate measurements, but conversion of 25% of the cysteine to the adduct at 0.25 mM cysteine would not be inconsistent with the data. Apparently, the decrease in rate of the Fe(III)/cysteine reaction as the PBN concentration exceeds 0.5 mM is due to the conversion of cysteine to an unreactive cysteine/PBN adduct. We infer that at 0.2 mM PBN (conditions typical of the kinetic experiments described next), conversion to the adduct is negligible.

Kinetic experiments to test as to whether PBN reacts with $[Fe^{III}(bpy)_2(CN)_2]^+$ were run by mixing equal volumes of 5.0×10^{-5} M $[Fe^{III}(bpy)_2(CN)_2]^+$ with 1.0×10^{-2} M PBN, in the presence of 1.0 mM $dipic^{2-}$ and 10.0 mM phosphate buffer (pH 7.56). The rate of the reaction between $[Fe^{III}(bpy)_2(CN)_2]^+$ and PBN is rather slow, with the half-life over 900 s. As the reaction of $[Fe^{III}(bpy)_2(CN)_2]^+$ with cysteine is much faster, the reaction of PBN with $[Fe^{III}(bpy)_2(CN)_2]^+$ can be neglected.

On the basis of the previous experimental results, 0.20 mM PBN was deemed sufficient to prevent inhibition by $[Fe^{II}(bpy)_2(CN)_2]$ and to be otherwise of no effect on the kinetics. Accordingly, this quantity of PBN was present in all further kinetic studies on this reaction.

In a test to determine as to whether L-cystine reacts with $[Fe^{III}(bpy)_2(CN)_2]^+$, a mixture was prepared with equal volumes of 2.5×10^{-4} M L-cystine and 2.5×10^{-5} M $[Fe^{III}(bpy)_2(CN)_2]^+$ at pH 7.94 (10 mM phosphate). The production of Fe(II) was very slow, with a half-life of at least 900 s. Thus, cystine is essentially inert on the time scale of the cysteine/Fe(III) reaction.

(55) Potapenko, D. I.; Bagryanskaya, E. G.; Tsentalovich, Y. P.; Reznikov, V. A.; Clanton, T. L.; Khramtsov, V. V. *J. Phys. Chem. B* **2004**, *108*, 9315−9324.

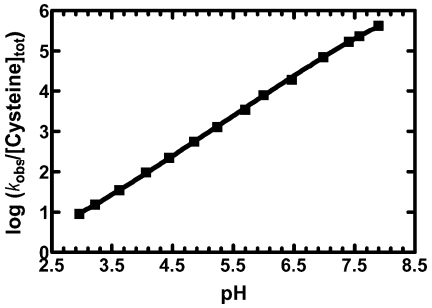

Figure 4. Plot of log(k_{obs}/[L-cysteine]$_{tot}$) vs pH for the oxidation of L-cysteine by $[Fe^{III}(bpy)_2(CN)_2]^+$, in the presence of 0.20 mM PBN and 1.0 mM dipic^{2-} at $\mu = 0.10$ M and 25.0 °C. Solid line shows the fit to eq 6 (weight by $(1/(k/[cys]))^2$).

A series of kinetic experiments was performed to determine the order of the reaction with respect to the cysteine concentration. The reactions were conducted by varying [L-cysteine]$_{tot}$ from 0.236 to 7.21 mM, with 2.5×10^{-5} M $[Fe^{III}(bpy)_2(CN)_2]^+$, 1.0 mM dipic^{2-}, 10.0 mM cacodylate buffer (pH 6.0), 0.20 mM PBN, and $\mu = 0.10$ M. In all cases, pseudo-first-order behavior over at least 3 half-lives was obtained, the values of pseudo-first-order rate constants (k_{obs}) being summarized in Table S-3 (Supporting Information). A plot of k_{obs} versus [L-cysteine]$_{tot}$ is shown in Figure 3. It is linear with a slope of $(7.25 \pm 0.09) \times 10^3$ M^{-1} s^{-1} and an intercept of (0.30 ± 0.05) s^{-1}. We suspect that the statistical significance of the nonzero intercept is questionable because of the potential of systematic errors to distort the data. With this caveat, the rate of the reaction has a first-order dependence on [L-cysteine]$_{tot}$ as in

$$k_{obs} = k[\text{L-cysteine}]_{tot} \quad (4)$$

The kinetic pH dependence was investigated in a series of experiments with the pH varied from 2.95 to 7.89, the resulting values of k_{obs} being summarized in Table S-4 (Supporting Information). A plot of log(k_{obs}/[L-cysteine]$_{tot}$) versus pH shown in Figure 4 indicates that log(k_{obs}/[L-cysteine]$_{tot}$) increases smoothly but nonlinearly as the pH increases. Cysteine exists principally as a neutral zwitterion (cys) at neutral pH, but it can be protonated to form a cation (cisH$^+$) in acidic media, and it can be deprotonated twice in alkaline media (cis$-$H$^-$ and cis$-$2H^{2-}). The three macroscopic proton dissociation equilibrium constants are as follows:[48] p$K_{a1} = 1.90$, p$K_{a2} = 8.18$, and p$K_{a3} = 10.30$. In principle, the four different forms of L-cysteine can react with $[Fe^{III}(bpy)_2(CN)_2]^+$ through kinetically distinguishable terms, as shown in eq 5

$$k_{obs} = \left\{\frac{k_1[H^+]^3 + k_2K_{a1}[H^+]^2 + k_3K_{a1}K_{a2}[H^+] + k_4K_{a1}K_{a2}K_{a3}}{[H^+]^3 + K_{a1}[H^+]^2 + K_{a1}K_{a2}[H^+] + K_{a1}K_{a2}K_{a3}}\right\}[\text{L} - \text{cysteine}]_{tot} \quad (5)$$

here, k_1 to k_4 represent the reactivity of protonated, neutral, monoanionic, and dianionic L-cysteine species, respectively. A nonlinear least-squares fit of the data in Table S-4 to eq 5 with the previous literature values for the K_a values yields statistically negligible values for k_1 and k_4. Excellent results were obtained with a fit to the simpler eq 6

$$k_{obs} = \left\{\frac{k_2K_{a1}[H^+]^2 + k_3K_{a1}K_{a2}[H^+]}{[H^+]^3 + K_{a1}[H^+]^2 + K_{a1}K_{a2}[H^+] + K_{a1}K_{a2}K_{a3}}\right\}[\text{L} - \text{cysteine}]_{tot} \quad (6)$$

The result of the fit is shown by the solid line in Figure 4. The obtained rate constants k_2 and k_3 are (3.4 ± 0.6) and $(1.18 \pm 0.02) \times 10^6$ M^{-1} s^{-1}.

Kinetics: $[Fe^{III}(bpy)(CN)_4]^-$. In view of the substantial kinetic inhibition by Fe(II) reported above for the reaction of $[Fe^{III}(bpy)_2(CN)_2]^+$ with cysteine, the analogous reaction of $[Fe^{III}(bpy)(CN)_4]^-$ was carefully examined for similar effects. In all of the kinetics experiments reported next, no significant deviations were detected in the pseudo-first-order fits. Moreover, deliberate addition of Fe(II) slowed the rates by only a small amount. Specifically, the addition of 50 μM Fe(II) increased the half-life from 20 to 25 s for the oxidation of 2.60×10^{-3} M L-cysteine by 5.0×10^{-5} M $[Fe^{III}(bpy)(CN)_4]^-$, with 10.0 mM cacodylate buffer (pH 5.98), 5.0 mM EDTA, and 0.093 M $NaClO_4$, and the addition of 100 μM Fe(II) increased the half-life to only 28 s. Evidently, kinetic inhibition by Fe(II) is insignificant in this reaction, at least under the pH conditions employed next and when Fe(II) is not added to the reaction.

A test was performed to determine as to whether L-cystine reacts with $[Fe^{III}(bpy)(CN)_4]^-$. Because of the low solubility of L-cystine at pH values between 3.0 and 7.0,[52,53] the following experiment was carried out at pH 8.0. No significant formation of Fe(II) was detected over 4800 s upon mixing equal volumes of 1.0×10^{-3} M L-cystine and 1.0×10^{-4} M $[Fe^{III}(bpy)(CN)_4]^-$, in the presence of 10.0 mM phosphate buffer.

The reduction of 5.0×10^{-5} M $[Fe^{III}(bpy)(CN)_4]^-$ was investigated as a function of L-cysteine concentration and pH, in the presence of 5.0 mM EDTA (pH $\leq$ 9.00), 10.0 mM EDTA (9.00 $<$ pH $\leq$ 10.0), and 1.0 mM cyclam (pH $>$ 10.0) at $\mu = 0.10$ M ($NaClO_4$). The rate of the reaction followed pseudo-first-order behavior over 3 half-lives, and the pseudo-first-order rate constants (k_{obs}, s^{-1}) from replicate runs agreed to better than $\pm$5%. A series of kinetic experiments was run with [L-cysteine]$_{tot}$ varying from 0.5 to 12 mM at pH 7.04 (10.0 mM cacodylate buffer), the values of k_{obs} being summarized in Table S-5 (Supporting Information). A plot of k_{obs} versus [L-cysteine]$_{tot}$ is shown in Figure 5; it is linear with a slope of $(1.11 \pm 0.02) \times 10^2$ M^{-1} s^{-1} and an intercept of $(8.44 \pm 26.1) \times 10^{-4}$ s^{-1}. The intercept value is statistically zero, so the rate of the reaction has a first-order dependence on [L-cysteine]$_{tot}$ as in eq 4.

A series of kinetic runs was performed with the pH varied from 6.09 to 11.9, the values of k_{obs} being summarized in Table S-6 (Supporting Information). The plot of (log k_{obs}/[L-cysteine]$_{tot}$) versus pH (Figure 6) reveals an irregularly monotonic increase in rate with increasing pH. A fit of the four-term expression in eq 5 to the data yields values for k_1 and k_2 indistinguishable from zero. Excluding both k_1 and

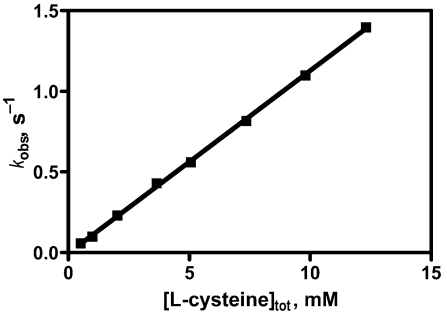

Figure 5. k_{obs} vs [L-cysteine]$_{tot}$ for the oxidation of L-cysteine by $[Fe^{III}(bpy)(CN)_4]^-$ at pH 6.92 (10.0 mM cacodylate buffer), in the presence of 5.0 mM EDTA at μ = 0.10 M (0.061 M $NaClO_4$) and 25.0 °C, $[Fe^{III}(bpy)(CN)_4^-]_0 = 5.0 \times 10^{-5}$ M. Solid line is a linear fit, weighted by $1/Y^2$.

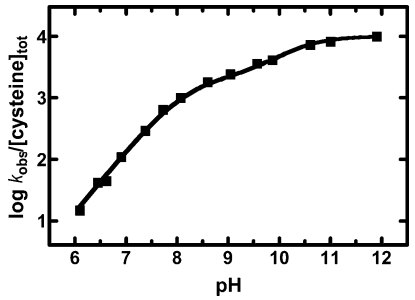

Figure 6. Plot of log(k_{obs}/[L-cysteine]$_{tot}$) vs pH for the oxidation of L-cysteine by $[Fe^{III}(bpy)(CN)_4]^-$ with 5.0 mM EDTA (pH from 6.0 to 9.0), 10.0 mM EDTA (pH from 9.0 to 10.0), or 1.0 mM cyclam (pH > 10.0), at an ionic strength of 0.10 M and 25.0 °C. Solid line shows the fit to eq 7 (weight by $(1/(k/[cys]))^2$).

k_2 terms as in eq 7 yields an excellent fit as shown in Figure 6, with k_3 and k_4 being $(2.13 \pm 0.08) \times 10^3$ M^{-1} s^{-1} and $(1.01 \pm 0.06) \times 10^4$ M^{-1} s^{-1}, respectively

$$k_{obs} = \left\{ \frac{k_3 K_{a1} K_{a2} [H^+] + k_4 K_{a1} K_{a2} K_{a3}}{[H^+]^3 + K_{a1}[H^+]^2 + K_{a1}K_{a2}[H^+] + K_{a1}K_{a2}K_{a3}} \right\} [\text{cysteine}]_{tot} \quad (7)$$

Specific cation effects might be anticipated to play a role in the kinetics of the reaction of $[Fe^{III}(bpy)(CN)_4]^-$ with the cys$-2H^{2-}$ dianion. A test for such effects was performed at pH 11.0 by substituting Li^+ for Na^+ in the oxidation of 5.1×10^{-4} M L-cysteine by 5.01×10^{-5} M $[Fe^{III}(bpy)(CN)_4]^-$ in the presence of 1.0 mM cyclam and 1.0 mM NaOH at μ = 0.10 M ($MClO_4$). The pseudo-first-order constants are 4.45 and 4.30 s^{-1}, respectively, thus demonstrating that specific cation effects are insignificant in this reaction.

Discussion

The oxidations of L-cysteine by $[Fe^{III}(bpy)_2(CN)_2]^+$ and $[Fe^{III}(bpy)(CN)_4]^-$ conform to the rule that outer-sphere thiol oxidations are strongly catalyzed by trace amounts of Cu^{2+}. The latter example is unusual in that it requires chelating agents stronger than dipic to achieve complete suppression of the copper catalysis. As Berthon has noted, the literature on the binding of cysteine by copper ions is somewhat confused by the occasional failure to recognize that Cu(II) is reduced to Cu(I) by cysteine.[56] Nevertheless, it is clear that Cu(I) has a very high affinity for cysteine, particularly in alkaline media. The requirement for more strongly binding sequestrants in the reaction of $[Fe^{III}(bpy)(CN)_4]^-$ may be a consequence of its relatively low $E°$ value and the higher pH values employed.

When appropriate ligands are present to achieve complete inhibition of catalysis by trace levels of copper, the direct oxidation of cysteine by the two Fe(III) complexes described here is proposed to have the following general mechanism:

$$^-SCH_2CH(NH_3^+)CO_2H + Fe(III) \rightleftharpoons {}^\bullet SCH_2CH(NH_3^+)CO_2H + Fe(II) \quad k_{cys}, k_{-cys} \quad (8)$$

$$^-SCH_2CH(NH_3^+)CO_2^- + Fe(III) \rightleftharpoons {}^\bullet SCH_2CH(NH_3^+)CO_2^- + Fe(II) \quad k_{cys-H}, k_{-cys-H} \quad (9)$$

$$^-SCH_2CH(NH_2)CO_2^- + Fe(III) \rightleftharpoons {}^\bullet SCH_2CH(NH_2)CO_2^- + Fe(II) \quad k_{cys-2H}, k_{-cys-2H} \quad (10)$$

$$RS^\bullet + \text{cys-H}^- \rightleftharpoons RSSR^{-\bullet} \quad k_R, k_{-R}, K_{rad} \quad (11)$$

$$RS^\bullet + PBN \rightarrow PBN/RS^\bullet \quad k_{PBN} \quad (12)$$

$$PBN/RS^\bullet + Fe(III) \rightarrow PBN/RS^+ + Fe(II) \quad \text{(fast)} \quad (13)$$

$$RSSR^{-\bullet} + Fe(III) \rightarrow RSSR + Fe(II) \quad k_d \text{ (fast)} \quad (14)$$

The first three steps in this mechanism correspond to outer-sphere electron transfer to Fe(III) from three of the protonation states of cysteine: cys, cys$-H^-$, and cys$-2H^{2-}$, respectively. The first two refer to specific tautomers in which the thiolate form is reactive, while the third is an obligate thiolate. Steps 11−14 are nonspecific regarding the protonation state, with $RS^\bullet$ designating the cysteinyl radical, $RSSR^{-\bullet}$ designating the radical anion of cystine, $PBN/RS^\bullet$ designating the PBN adduct of the cysteinyl radical, and RSSR designating cystine.

The tautomerization equilibria of cys and cys$-H^-$ are well-understood.[57,58] The neutral state exists predominantly as $HSCH_2CH(NH_3^+)CO_2^-$, as well as small amounts of $^-SCH_2CH(NH_3^+)CO_2H$ and $HSCH_2CHNH_2CO_2H$ ($pK_i = 5.5$ and $pK_{ii} = 4.88$)[58]

$$HSCH_2CH(NH_3^+)CO_2^- \rightleftharpoons {}^-SCH_2CH(NH_3^+)CO_2H \quad K_i \quad (15)$$

$$HSCH_2CH(NH_3^+)CO_2^- \rightleftharpoons HSCH_2CH(NH_2)CO_2H \quad K_{ii} \quad (16)$$

$^-SCH_2CH(NH_3^+)CO_2^-$ is the major form of monoanionic cysteine, and the minor tautomers are $HSCH_2CHNH_2CO_2^-$ and $^-SCH_2CHNH_2CO_2H$. The equilibrium constant for the

(56) Berthon, G. *Pure Appl. Chem.* **1995**, *67*, 1117−1240.
(57) Friedman, M. *The Chemistry and Biochemistry of the Sulfhydryl Group in Amino Acids, Peptides, and Proteins*; Pergamon Press: New York, 1973; p 4.
(58) Kallen, R. G. *J. Am. Chem. Soc.* **1971**, *93*, 6227−6235.

Table 6. Kinetic Parameters for the Oxidation of L-Cysteine by the Two Fe(III) Complexes[a]

parameter	oxidant	
	$[Fe^{III}(bpy)_2(CN)_2]^+$	$[Fe^{III}(bpy)(CN)_4]^-$
$2k_{cys}$ (M^{-1} s^{-1})	$(1.1 \pm 0.2) \times 10^6$	
$2k_{cys-H}$ (M^{-1} s^{-1})	$(1.18 \pm 0.02) \times 10^6$	$(2.13 \pm 0.08) \times 10^3$
$2k_{cys-2H}$ (M^{-1} s^{-1})		$(1.01 \pm 0.06) \times 10^4$
log K_{cys}[b]	-4.1 ± 1.7	-7.8 ± 1.7
K_{cys-H}[b]	9.0×10^{-3}	1.6×10^{-6}
K_{cys-2H}[b]	9.6×10^{-1}	1.7×10^{-4}
$2k_{-cys}$ (M^{-1} s^{-1})[c]	1.4×10^{10}	
$2k_{-cys-H}$ (M^{-1} s^{-1})[c]	1.3×10^8	1.3×10^9
$2k_{-cys-2H}$ (M^{-1} s^{-1})[c]		5.9×10^7

[a] In anaerobic aqueous solution at 25.0 °C with $\mu = 0.10$ M. [b] Calculated from the standard potentials. [c] Calculated from the ratio of the forward rate constant and the equilibrium constant.

tautomerization of the monoanion to the thiol form is 0.40, while the equilibrium constant to the carboxylic acid form is quite small ($K = 6.02 \times 10^{-6}$).[58]

Under conditions where the back electron-transfer steps in eqs 8−10 can be neglected and no PBN is present, application of the steady-state approximation to the radical species leads to the general rate law

$$\frac{-\mathrm{d[Fe(III)]}}{\mathrm{d}t} = 2\left\{\frac{k_{cys}K_{a1}K_i[H^+]^2 + k_{cys-H}K_{a1}K_{a2}[H^+] + k_{cys-2H}K_{a1}K_{a2}K_{a3}}{[H^+]^3 + K_{a1}[H^+]^2 + K_{a1}K_{a2}[H^+] + K_{a1}K_{a2}K_{a3}}\right\}[\mathrm{cysteine}]_{tot}[\mathrm{Fe(III)}] \quad (17)$$

The same rate law is obtained when PBN is present and scavenges all the cysteinyl radicals. By comparing eq 17 to eq 6 (the empirical rate law for $[Fe^{III}(bpy)_2(CN)_2]^+$), it is evident that $2k_{cys}K_i$ is k_2 (3.4 ± 0.6 M^{-1} s^{-1}), $2k_{cys-H}$ is k_3 ($(1.18 \pm 0.02) \times 10^6$ M^{-1} s^{-1}), and k_{cys-2H} is not detected. With $pK_i = 5.5$ as mentioned previously, this yields $2k_{cys} = (1.1 \pm 0.2) \times 10^6$ M^{-1} s^{-1}. Similarly, with $[Fe^{III}(bpy)(CN)_4]^-$ as the oxidant, eq 7 reveals that k_{cys} is not detected, $2k_{cys-H}$ is $(2.13 \pm 0.08) \times 10^3$ M^{-1} s^{-1}, and $2k_{cys-2H}$ is k_4 ($(1.01 \pm 0.06) \times 10^4$ M^{-1} s^{-1}). A listing of these rate constants is given in Table 6.

A challenging question is understanding why overoxidation to cysteine-sulfinate (RSO_2^-) occurs in the oxidation of cysteine by $[Mo(CN)_8]^{3-}$ but not with the two current Fe(III) oxidants.[15] A similar puzzle is posed in the oxidations of TGA, where overoxidation to the sulfonate (RSO_3^-) occurs with $[IrCl_6]^{2-}$ but not with $[Mo(CN)_8]^{3-}$.[24,26] In both cases, overoxidation is believed to occur through reaction of the thiyl radical with the oxidant, leading to the sulfenic acid (RSOH), and certainly the competition of this step with eq 11 (association of the thiyl radical with the thiol) is an important consideration. A further complication is that to generate stable overoxidation products, the sulfenic acid must undergo further oxidation rather than comproportionation with the thiol. The current data seem to suggest that the stronger oxidants are more likely to generate overoxidation products, but it is likely that other factors are also significant, such as electrostatics, self-exchange rates, pH, and concentration ratios.

Qualitatively, the kinetic inhibition by Fe(II) observed in both current reactions can be understood as arising from the reversibility of the initial electron-transfer steps (eqs 8−10). A quantitative account of the inhibition can be easily achieved when the reverse rate constants are adjusted ad libitum, but if inhibition is achieved with the actual reverse rate constants, then such an account provides great support for the mechanism proposed. In the present study, the reverse rate constants can be calculated from the forward rate constants and the standard (or formal) potentials of the reactants. The formal potentials of the two Fe(III) oxidants used in this study can be approximated as the $E_{1/2}$ values given in Table 1. We have previously reported that $E°$ is 0.76 ± 0.02 V for reduction of the cysteinyl radical in alkaline media as in eq 18[15]

$$^{\bullet}SCH_2CH(NH_2)CO_2^- + e^- = {}^-SCH_2CH(NH_2)CO_2^- \quad (18)$$

According to Mezyk and Armstrong, the cysteinyl radical is protonated at the amine site near neutral pH, the pK_a being 8.26 ± 0.04;[59] the microscopic dissociation constant (pK_{SNN}) of $^-SCH_2CH(NH_3^+)CO_2^-$ is 10.36. By combining these acid dissociation constants with the alkaline cysteinyl radical potential mentioned previously, we derive $E° = 0.88 \pm 0.02$ V for the reduction of $^{\bullet}SCH_2CH(NH_3^+)CO_2^-$ to $^-SCH_2CH(NH_3^+)CO_2^-$. If it is assumed that the 0.12 V shift in potential that occurs by protonation of the amine implies a similar 0.12 V shift for protonation at the carboxylate, then a rough estimate of $E° = 1.00$ V can be derived for the reduction of $^{\bullet}SCH_2CH(NH_3^+)CO_2H$ to $^-SCH_2CH(NH_3^+)CO_2H$; the crude nature of this method of estimation suggests an uncertainty of ± 0.1 V in $E°$. These reduction potentials lead to the equilibrium constants for reactions 7−9 (K_{cys}, K_{cys-H}, and K_{cys-2H}) that are shown in Table 6. Values for the reverse rate constants (k_{-cys-H} and $k_{-cys-2H}$) are then calculated from the ratio of the forward rate constants and the equilibrium constants and are given in Table 6. It can be seen that these reverse rate constants are quite large, as they must be if they are to lead to kinetic inhibition, and their validity is supported by the observation that none exceeds the limits of diffusion control.

The degree of kinetic inhibition by Fe(II) predicted by the previous mechanism is also quite sensitive to the magnitude of the equilibrium constant K_{rad}. This sensitivity arises because the equilibrium constant is not very large, so that in nonalkaline media, the majority of the cysteine radicals is present as the cysteinyl radical rather than the disulfide radical anion. Irreversible removal of the radicals through oxidation of the disulfide radical ion (eq 14) thus depletes the radicals at a rate that depends on $K_{rad.}$ The magnitude of K_{rad} is pH dependent because it depends on the state of protonation of the amines.[59] Unfortunately, the pH dependence has been measured only at pH 6 and above; Mezyk and Armstrong's fit of the pH dependence yielded $K_{p2} = 8900$ M^{-1}, which is the equilibrium constant for the reaction

(59) Mezyk, S. P.; Armstrong, D. A. *J. Chem. Soc., Perkin Trans. 2* **1999**, 1411−1419.

$$\text{cys-H}^- + \text{RS}^\bullet \rightleftharpoons \text{RSSR}^{\bullet -} \quad K_{p2} \tag{19}$$

under conditions where both amines in the reactants are protonated. With the relationship $K_{rad} = K_{a2}K_{p2}$, we calculate $K_{rad} = 5.8 \times 10^{-5}$. It is a considerable extrapolation to use this result at pH 3.2, where our data on kinetic inhibition in the reaction with $[Fe(bpy)_2(CN)_2]^+$ were obtained. In fact, it proved necessary to adjust K_{rad} to 1.5×10^{-2} to obtain optimal agreement with the experimental results, as described next. Protonation at the carboxylates was not included in Mezyk and Armstrong's fit; if this were significant for $RSSR^{\bullet -}$ at pH 3.2, it could explain the shift in K_{rad} required in our kinetic modeling.

Simulations of the kinetic inhibition by Fe(II) in the reaction of $[Fe(bpy)_2(CN)_2]^+$ with cysteine at pH 3.2 were performed by the use of the Specfit/32 computer program. The kinetic model, which is a simplified version of the mechanism in eqs 8−14 (detailed in Table S-7, Supporting Information), consists of K_{a1} and K_{a2} (the first two acid dissociation reactions of cysteine, treated as rapid equilibria), the reversible oxidation of cys-H^- by Fe(III) (eq 9, which is the major pathway at this pH), reaction 11 (association of cysteine with the cysteinyl radical, treated as a rapid equilibrium), and the irreversible oxidation of the cystine radical anion (reaction 14). The agreement between the measured and the calculated half-lives was taken as the measure of success of the simulations. Essentially, perfect results were obtained with the small adjustment of k_{cys-H} to $8.1 \times 10^5\ M^{-1}\ s^{-1}$ to compensate for the neglect of the minor pathway k_{cys}. When the bimolecular recombination of the cysteinyl radicals was added to the previous mechanism with a rate constant of $10^{10}\ M^{-1}\ s^{-1}$, there was no effect on the simulations, thus showing that the major fate of the radicals is best described by association to form the cystine radical anion and its oxidation to cystine.

Simulations of the oxidation of cysteine by $[Fe(bpy)(CN)_4]^-$ were performed likewise, with a model consisting of K_{a2} and K_{a3}, the reversible oxidation of cys−H^- by Fe(III), K_{rad}, and the irreversible oxidation of the cystine radical anion by Fe(III). Essentially, perfect simulation of the inhibition by Fe(II) (described previously) was achieved with this model (Table S-8, Supporting Information). This simulation was performed with the adjusted value for K_{rad} mentioned previously, but substantially smaller values could be accommodated by increasing the rate constant for reaction of Fe(III) with the cystine radical anion. Again, inclusion of bimolecular recombination of the cysteinyl radicals had no effect on the simulations. In summary, the mechanism in eqs 8−14 accounts quantitatively for the kinetic inhibition by Fe(II) for both reactions discussed herein. The reason that bimolecular recombination of the cysteinyl radicals is insignificant, even under acidic conditions, is that the steady-state concentration of the radicals is very low, and thus, the second-order recombination does not compete with the pseudo-first-order oxidation of the cystine radical anion.

The effectiveness of PBN in preventing kinetic inhibition by Fe(II) is attributed to its rapid scavenging of the cysteinyl radicals as in eq 12. PBN is well-known to scavenge cysteinyl radicals,[54] but the rate constant appears not to have been determined. The analogous reaction of the cysteinyl radical with DMPO has a rate constant of $2.10 \times 10^8\ M^{-1}\ s^{-1}$,[60] so a similar rate constant might be anticipated for PBN. If this were the case, then the rate constant would be comparable to that for reaction of the cysteinyl radical with Fe(II), and thus, it is understandable as to why significantly higher concentrations of PBN than $[Fe(bpy)_2(CN)_2]$ are required to achieve complete scavenging. At higher pH values, the position of equilibrium is shifted to the right for the reaction of cysteine radicals with cysteine (K_{rad}), and so kinetic inhibition is insignificant, even in the absence of PBN.

Our proposed general mechanism includes three rate-limiting steps, eqs 8−10. Each of these rate-limiting steps is a simple electron-transfer process, differing from each other only by the cysteine protonation state. As no substitution occurs at the transition metal centers, it is reasonable to consider as to whether these steps are properly described as having outer-sphere electron-transfer mechanisms. One test of this description is to apply the cross-relationship of Marcus theory. Suitable self-exchange reactions for the cysteine species must be defined as simple reversible degenerate bimolecular electron-transfer reactions: the specific tautomeric forms of cysteine and their corresponding radicals shown in each of reactions 8−10 have been selected to satisfy these requirements, and they lead to a set of three self-exchange rate constants that are pH independent. In the following discussion, we apply these concepts to steps 9 and 10 (k_{cys-H} and k_{cys-2H}) but not to step 8 (k_{cys}) because the parameters relating to the latter are less certain.

The value of k_{cys-2H} obtained from the reaction of $[Fe(bpy)(CN)_4]^-$ can be used to derive the self-exchange rate constant of the $^\bullet SCH_2CH(NH_2)CO_2^-/^-SCH_2CH(NH_2)CO_2^-$ couple. The following equations from Marcus theory are used:[61]

$$k_{12} = (k_{11}k_{22}K_{12}f_{12})^{1/2}W_{12} \tag{20}$$

$$\ln f_{12} = \frac{[\ln K_{12} + (w_{12} - w_{21})/RT]^2}{4[\ln(k_{11}k_{22}/Z^2) + (w_{11} + w_{22})/RT]} \tag{21}$$

$$W_{12} = \exp(-w_{12} - w_{21} + w_{11} + w_{22})/2RT \tag{22}$$

$$w_{ij} = 4.23Z_iZ_j/[r(1 + 0.328r\sqrt{\mu})] \tag{23}$$

In these equations, k_{12} is the observed cross-electron-transfer rate constant ($5.0 \times 10^3\ M^{-1}\ s^{-1}$), and k_{11} and k_{22} are the self-exchange rate constants of the $^\bullet SCH_2CH(NH_2)CO_2^-/^-SCH_2CH(NH_2)CO_2^-$ and $[Fe(bpy)(CN)_4]^{-/2-}$ redox couples. Z is the collision frequency, for which a value of $1 \times 10^{11}\ M^{-1}\ s^{-1}$ is used in our calculations. Z_i and Z_j are the ionic charges on the reactants, R is the ideal gas constant (1.987×10^{-3} kcal mol^{-1}), and r is the center-to-center distance between reactants while in contact.

(60) Davies, M. J.; Forni, L. G.; Shuter, S. L. *Chem.-Biol. Interact.* **1987**, *61*, 177−188.
(61) Zuckerman, J. J. *Inorganic Reactions and Methods*; VCH: Deerfield Beach, FL, 1986; Vol. 15, pp 13−47.

A value of the self-exchange rate constant ($k_{22} = 4 \times 10^7$ M^{-1} s^{-1}) of the $[Fe(bpy)(CN)_4]^{-/2-}$ redox couple was derived by Stasiw and Wilkins from the rate of oxidation of $[Fe(bpy)(CN)_4]^{2-}$ by $[Fe(CN)_6]^{3-}$.[31] However, charge effects were not included in the calculation, and the self-exchange reaction of $[Fe(CN)_6]^{3-/4-}$ is now known to be catalyzed by alkali metal ions.[62,63] To avoid these complications, we estimate k_{22} by applying Marcus' equations to the oxidation of L-ascorbate by $[Fe(phen)(CN)_4]^-$ as in reaction 24[30,45,61,64]

$$[Fe(phen)(CN)_4]^- + HA^- \rightarrow [Fe(phen)(CN)_4]^{2-} + HA^{\bullet} \quad (24)$$

This reaction was studied at $\mu = 1.0$ M, and a rate constant of 4×10^4 M^{-1} s^{-1} was obtained.[30] The reduction potential of the $[Fe(phen)(CN)_4]^{-/2-}$ couple is pH dependent,[65] presumably because the Fe(II) species is weakly basic.[66] From the pH dependent electrochemical data of Schilt and Cresswell, a value of $E_f = 0.61$ V can be inferred for the unprotonated species at $\mu = 1.0$ M.[65] Given 0.71 V as $E_f(HA^{\bullet}/HA^-)$,[64] a value of 0.02 is calculated for the equilibrium constant of reaction 24. The self-exchange rate constant for the $HA^{\bullet}/HA^-$ couple is taken as 1×10^5 M^{-1} s^{-1},[64] and the radii of $[Fe(phen)(CN)_4]^-$ and HA^- are taken as 5.33 and 3.00 Å, respectively.[30,45] Using the previous known parameters, the self-exchange rate constant of $[Fe(phen)(CN)_4]^{-/2-}$ is recalculated as 6×10^5 M^{-1} s^{-1}, and it is assumed that the same value applies to the self-exchange rate constant (k_{22}) of the $[Fe(bpy)(CN)_4]^{-/2-}$ redox couple. This value of k_{22} along with a value of 1.70×10^{-4} for K_{12} (K_{cys-2H}), and the radii of $[Fe(bpy)(CN)_4]^-$ and $^-SCH_2CH(NH_2)CO_2^-$ (5.33 and 3.00 Å, respectively),[15,45] lead to a calculated self-exchange rate constant of $^{\bullet}SCH_2CH(NH_2)CO_2^-/^-SCH_2CH(NH_2)CO_2^-$, k_{11}, of 4.5×10^5 M^{-1} s^{-1}. A smaller value for k_{11} was derived from the reaction of $[Mo(CN)_8]^{3-}$ with L-cysteine ($k_{11} = 5.4 \times 10^3$ M^{-1} s^{-1}).[15] The latter value, however, was derived through neglect of the specific cation effect in this reaction's rate law, and so the k_{11} value derived from the current reaction is considered to be more reliable.

The Marcus cross-relationship can also be applied to k_{cys-H} (determined for both $[Fe(bpy)(CN)_4]^-$ and $[Fe(bpy)(CN)_2]^+$) to derive an estimate of k_{11} for the protonated couple $^{\bullet}SCH_2CH(NH_3^+)CO_2^-/^-SCH_2CH(NH_3^+)CO_2^-$. In a straightforward calculation with the parameters given previously and in Table 6, a value for k_{11} of 5×10^6 M^{-1} s^{-1} was obtained from the reaction of $[Fe(bpy)(CN)_4]^-$. A similar calculation of k_{11} from the reaction of $[Fe(bpy)_2(CN)_2]^+$ with cystine required a k_{22} value for this oxidant: we derived a value for k_{22} of 4×10^6 M^{-1} s^{-1} by applying Marcus' equations to the oxidation of L-ascorbate by $[Fe(bpy)_2(CN)_2]^+$.[30,45,61,64] This calculation is based on a rate constant of 3.2×10^6 M^{-1} s^{-1} at $\mu = 1.0$ M for the oxidation of ascorbate by $[Fe(bpy)_2(CN)_2]^+$,[30] $E_f = 0.78$ V for $[Fe(bpy)_2(CN)_2]^{+/0}$ at $\mu = 1.0$ M,[44] radii of 6.77 Å for $[Fe(bpy)_2(CN)_2]^+$ and 3.00 Å for $^-SCH_2CH(NH_3^+)CO_2^-$ estimated from CPK models,[15,45] and other parameters as given previously. By using the previous known parameters, the self-exchange rate constant of $^{\bullet}SCH_2CH(NH_3^+)CO_2^-/^-SCH_2CH(NH_3^+)CO_2^-$, k_{11}, is calculated as 7×10^6 M^{-1} s^{-1}, in excellent agreement with that obtained from the oxidation of L-cysteine by $[Fe(bpy)(CN)_4]^-$. Apparently, protonation at the amine site leads to a 15-fold increase in the cysteine self-exchange rate constant. This rate increase is attributed to a decrease in electrostatic repulsion between the reactants. For both self-exchange reactions, the rate constants are rather large, as is to be expected from the small structural changes that accompany the formation of cysteine radicals.[67] Overall, these satisfactory results provide evidence that both the k_{cys-H} and the k_{cys-2H} pathways are well-described as outer-sphere electron-transfer processes.

Very recently, a substantial kinetic isotope effect was observed in the oxidation of hydroxylamine by hexachloroiridate(IV).[68] This kinetic isotope effect was ascribed to concerted proton-coupled electron transfer (CPET), with the neutral form of hydroxylamine being the electron donor and the solvent (water) being the proton acceptor. It is conceivable that an analogous mechanism occurs in the oxidation of neutral L-cysteine by $[Fe^{III}(bpy)_2(CN)_2]^+$ as in eq 25

$$HSCH_2CH(NH_3^+)CO_2^- + [Fe(bpy)_2(CN)_2]^+ \rightarrow {}^{\bullet}SCH_2CH(NH_3^+)CO_2^- + Fe(bpy)_2(CN)_2 + H^+ \quad k_c \quad (25)$$

Its rate constant, k_c, would correspond to half of k_2 in eq 6, with (1.7 ± 0.3) M^{-1} s^{-1} for k_c. The relevant standard potential is calculated by using the standard potential of $RS^{\bullet}/RS^-$ ($E_f = 0.88$ V vs NHE) and the dissociation constant of neutral cysteine ($pK_{a2} = 8.18$), with $E_f(RS^{\bullet},H^+/RSH) = 1.36$ V versus NHE. On the basis of the half-wave potential of $[Fe(bpy)_2(CN)_2]^{+/0}$ and $E_f(RS^{\bullet},H^+/RSH)$, the $\Delta G°$ value for eq 25 is 58 kJ mol^{-1}. Although this CPET mechanism is not ruled out, the high $\Delta G°$ value of eq 25 implies that this process is unfavorable. The similar values obtained for k_{cys} and k_{cys-H} imply that both paths have the same mechanism; since k_{cys-H} is clearly an electron-transfer process, the same should apply to k_{cys}, and CPET can be disregarded. In contrast to electron transfer being favored for cysteine oxidation, CPET may be the favored pathway in the oxidation of H_2NOH because $\Delta G°$ is not unfavorable.

Ison et al. recently reported on the oxidation of cysteine by ClO_2 between pH 3.3 and 6.[69] This reaction displays many characteristics that are similar to those reported herein, including a strong rate inhibition by acid. Only a single term in the rate law was detected, and it was attributed to the one-electron oxidation of the cysteine monoanion. These results plus our present and prior[15] results thus contribute to

(62) Macartney, D. H. *Inorg. Chem.* **1991**, *30*, 3337−3342.
(63) Zahl, A.; van Eldik, R.; Swaddle, T. W. *Inorg. Chem.* **2002**, *41*, 757−764.
(64) Macartney, D. H.; Sutin, N. *Inorg. Chim. Acta* **1983**, *74*, 221−228.
(65) Schilt, A. A.; Cresswell, A. M. *Talanta* **1966**, *13*, 911−918.
(66) Schilt, A. A. *J. Am. Chem. Soc.* **1963**, *85*, 904−908.
(67) van Gastel, M.; Lubitz, W.; Lassmann, G.; Neese, F. *J. Am. Chem. Soc.* **2004**, *126*, 2237−2246.
(68) Makarycheva-Mikhailova, A. V.; Stanbury, D. M.; McKee, M. L. *J. Phys. Chem. B* **2007**, *111*, 6942−6948.
(69) Ison, A.; Odeh, I. N.; Margerum, D. W. *Inorg. Chem.* **2006**, *45*, 8768−8775.

a growing consensus that one-electron oxidation of cysteine generally occurs only when the molecule is in its thiolate form.

Conclusion

As is typical of thiol oxidations, the oxidations of L-cysteine by $[Fe(bpy)_2(CN)_2]^+$ and $[Fe(bpy)(CN)_4]^-$ in anaerobic aqueous solution are strongly catalyzed by copper ions. With the addition of suitable inhibitors, the uncatalyzed reactions can be investigated as was the case also with $[Mo(CN)_8]^{3-}$. In contrast to the latter reaction, cystine is the sole sulfur-containing product with the two Fe(III) oxidants. The rate laws for both oxidants are first order in [cysteine] and [Fe(III)] and have complex pH dependences. They also both display mild kinetic inhibition by Fe(II), and in contrast with the Mo(V) reaction, they show no specific cation effects. A general mechanism is inferred in which the rate-limiting steps all entail reversible electron transfer from various protonation states of the thiolate forms of cysteine. The electron-transfer rate constants are consistent with the cross-relationship of Marcus theory when self-exchange rate constants of 6×10^6 and 4×10^5 M^{-1} s^{-1} are used for the $^{\bullet}SCH_2CH(NH_3^+)CO_2^-/^-SCH_2CH(NH_3^+)CO_2^-$ and $^{\bullet}SCH_2CH(NH_2)CO_2^-/^-SCH_2CH(NH_2)CO_2^-$ redox couples. These results provide a basis for the general prediction of rates of outer-sphere oxidation of cysteine.

Acknowledgment. The authors thank the National Science Foundation (NSF) for funding this research under Grant 0509889. Any opinions, findings, conclusions, or recommendations expressed in this material are those of the author(s) and do not necessarily reflect the views of the NSF. The authors also thank Song Na for performing tests on the reaction of PBN with cysteine, Prof. Peter Livant (Auburn University) for assisting us in running NMR spectra, and Prof. Doug Goodwin (Auburn University) for the use of his Applied Photophysis stopped-flow instrument.

Supporting Information Available: Tables S-1−S-8 and Figures S-1−S-9. This material is available free of charge via the Internet at http://pubs.acs.org.

IC701891M